Structure of Phosphorus-Containing Peptide Ligands. X-ray and NMR Structural Study of Free Ligand and Rhodium Complex

Scott R. Gilbertson,*[,†] Guohua Chen,[†] Jeff Kao,[†] Alicia Beatty,[†] and Charles F. Campana[‡]

Department of Chemistry, Washington University, St. Louis, Missouri 63130 and Siemens Analytical X-ray Systems, Inc., 6300 Enterprise Lane, Madison, Wisconsin 53719-1173

Received April 30, 1997[⊗]

The structure of a series of phosphorus-containing peptides was studied. The X-ray structure of a phosphorus-containing dodecapeptide is reported. Analysis of the solution structure of similar phosphorus-containing peptides before and after coordination of rhodium is also reported. In both the solid state and in solution, the peptides were found to exist in a mixture of α-helical and 3_{10} helical conformations. Coordination of rhodium to the *i*, *i* + 4 orientated phosphine groups appears to alter the conformational preference.

Introduction

We recently reported the synthesis of phosphine-containing derivatives of serine.[1,2] In those papers we developed chemistry that allows for the protection of the potentially air sensitive phosphine group and its deprotection after incorporation into peptides. This chemistry was developed with two goals in mind. We feel that peptides with stable secondary structures should be excellent scaffolds upon which catalytically active transition metals can be placed. Such an arrangement has potential in the design and synthesis of catalysts that exhibit a variety of selectivities. The other motive behind the development of such a system is that large libraries of peptides can be made by combinatorial methods.[3−9] Consequently, the system we reported allows for the synthesis of large libraries of ligands which can coordinate transition metals and then be screened for unique activity and selectivity. This approach to ligand development cannot only lead to better ligands, but also add in an empirical way to the understanding of what features are important in a given catalytic system. Before either of these goals can be achieved, it is necessary to be able to characterize the phosphine−peptide ligand systems and their metal complexes. This paper reports the structural characterization of the first peptide system we developed.

The peptide reported in our first paper was designed to possess a helical structure through the predominant use of alanine and the incorporation of a number of aminoisobutyric acid (Aib) residues. After synthesis, the phosphine−sulfide side chains of this peptide were converted to free phosphines, and rhodium was bound into this unique environment. The secondary structure of that peptide and peptide−metal complex was assumed to be helical based on primary sequence and the peptide's ability to act as a bis-chelating ligand. The phosphine-containing amino acids were positioned in an *i*, *i* + 4 relationship which requires an α-helical secondary structure for the side chains to be in position to bind rhodium. While metal coordination was evidence for helical secondary structure it was not proof. It is conceivable that some other structure could have existed that allowed coordination to rhodium. Despite the binding of rhodium in one location, the structure of the remainder of the peptide chain was not conclusively demonstrated. This paper reports the X-ray crystal structure of our original phosphorus-containing peptide. Also reported is an NMR study of the secondary structure of a related peptide and a peptide−metal complex.

Results

Synthesis of Peptides. The desired peptides were synthesized by solid phase peptide chemistry. A segmental approach was taken, where the phosphine sulfide containing amino acid was incorporated as a dimer with alanine (**1**), and amino isobutyric acid was incorporated as either a dimer with alanine (**2**) or a trimer with alanine (**3**). The couplings were performed using either Wang or Rink resin depending on whether the acid or amide terminal peptide was desired.

X-ray Crystal Structure of Peptide 4. The inital peptide that was synthesized was a dodecamer that contained three Aib residues (**4**). This peptide was synthesized by standard FMOC peptide chemistry, incorporating two of the unnatural amino acid (diphenylphosphino)serine (Pps), in an *i*, *i* + 4 orientation.[1] X-ray quality crystals of this peptide were obtained by slow evaporation of a mixture of methanol, ethyl acetate, and hexane.

The X-ray crystallographic structure (Figure 2) shows peptide **4** existed in a right-handed helical conformation. This conformation was more apparent when the molecule was viewed along its axis from the amine terminus (Figure 2). A detailed study of the crystal structure revealed that the peptide was a mixture of 3_{10} and α-helix conformations. From Figure 2 one can see that the first several residues were in a 3_{10}-helical conformation. The residues in the middle of the sequence were α-helical, which was indicated by the location of the phosphine sulfides on the same side of the helix, given their *i*, *i* + 4 relationship. Figure 2 also clearly illustrates that the last two residues, at the acid terminus, were in an extended form.

---

† Washington University.
‡ Siemens Analytical X-ray Systems.
⊗ Abstract published in *Advance ACS Abstracts,* July 15, 1997.

(1) Gilbertson, S. R.; Chen, G.; McLoughlin, M. *J. Am. Chem. Soc.* **1994**, *116*, 4481.
(2) Gilbertson, S. R.; Wang, X. *J. Org. Chem.* **1996**, *61*, 434.
(3) Gilbertson, S. R.; Wang, X. *Tetrahedron Lett.* **1996**, *37*, 6475.
(4) Borman, S. *Chem. Eng. News* **1996**, Feb 12, 29.
(5) Baum, R. M. *Chem. Eng. News* **1994**, Feb 7, 20.
(6) Gordon, E. M.; Gallop, M. A.; Patel, D. V. *Acc. Chem. Res.* **1996**, *29*, 144.
(7) DeWitt, S. H.; Czarnik, A. W. *Acc. Chem. Res.* **1996**, *29*, 114.
(8) Nielsen, J. *Chem. Ind.* **1994**, *22*, 902.
(9) Ellman, J. A. *Acc. Chem. Res.* **1996**, *29*, 132.

S0022-3263(97)00773-1 CCC: $14.00

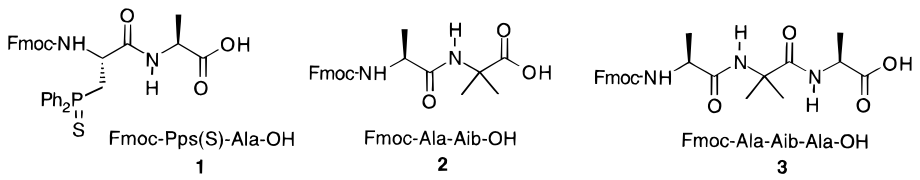

Figure 1.

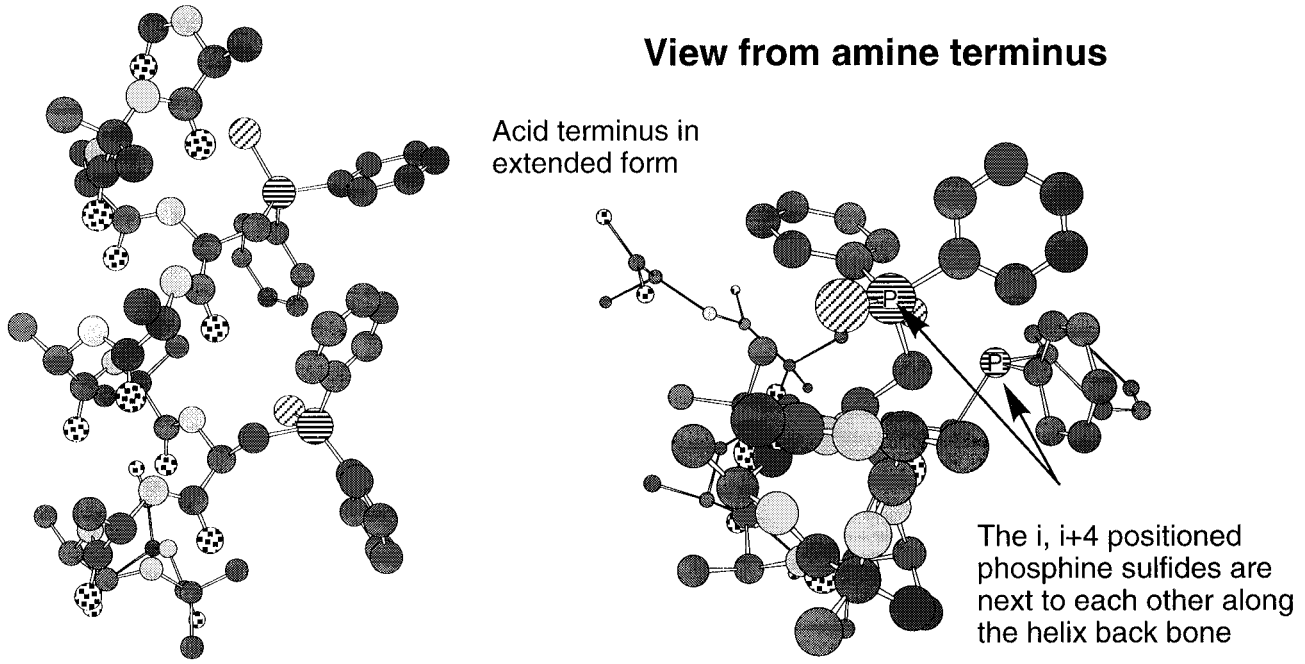

Figure 2. X-ray structure of **4** Ac-Ala-Aib-Ala-Pps(S)-Ala-Ala-Aib-Pps(S)-Ala-Ala-Aib-Ala-OH. The hydrogen atoms were omitted for clarity.

Table 1. Torsion Angles ϕ and ψ from X-ray Crystallographic Data of 4

	Ala[1]	Aib[2]	Ala[3]	Pps[4]	Ala[5]	Ala[6]	Aib[7]	Pps[8]	Ala[9]	Ala[10]	Aib[11]	Ala[12]
ϕ (deg)	−52.5	−56.5	−60.4	−74.1	−64.1	−65.9	−54.8	−71.7	−69.8	−82.0	+51.9	−167
ψ (deg)	−36.7	−29.5	−26.2	−24.9	−39.9	−47.2	−46.3	−32.2	−31.3	−15.0	+40.7	/[a]

[a] Not applicable.

These general observations are in agreement with analysis of the torsion angles ϕ and ψ of each residue and the hydrogen bonding pattern in the peptide backbone. The torsion angles ϕ and ψ for each residue from the X-ray crystallographic data of **4** are summarized in Table 1. The torsion angles ϕ and ψ for residues 1 to 10 were within the ranges defined for α-helix or a 3_{10} helix. The values of ϕ and ψ for the first three residues were close to the defined value for an ideal 3_{10}-helix, $\{\phi, \psi\} = \{-60°, -30°\}$, and the values for residues in the middle (residues 5, 6, and 7) were close to the defined value for an ideal α-helix, $\{\phi, \psi\} = \{-60°, -45°\}$.[10−12]

Marshall[13,14] and Burgess[15] have shown that the allowable ϕ and ψ angles for the Aib residue occur in two very restricted regions near −57°, −47° and +57°, +47°. These two regions corresponded to a right-handed α or 3_{10}-helix and a left-handed α or 3_{10}-helix, respectively. Toniolo *et al.* found that in an Aib decamer, the average value of ϕ was 54° and that of ψ was 31°.[10] The values, from the X-ray, of ϕ and ψ for Aib(2) and Aib(7) are consistent with a helical conformation. The positive value for ϕ and ψ observed for Aib(11) indicates a helix reversal, as is often the case at the carboxy end of Aib-containing peptides. This causes the end of the molecule to be in an extended conformation.[16,17]

The hydrogen bonds between the amide protons and carbonyl oxygen atoms also indicate a mixture of helix types. From the acetyl group to Ala(10) there were four 4-1 type (i, $i + 3$ type) hydrogen bonds interspersed with five 5-1 type (i, $i + 4$ type) hydrogen bonds. This was evidence that the peptide was a mixture of 3_{10} and α-helix structures. Three of the four 4-1 type hydrogen bonds were at the amine end and the other one was near the acid terminus, further indicating that the peptide had 3_{10}-helical character at the amine end.

Since we ultimately desired to bind transition metals to the phosphorus ligands in the side chains, we were very interested in the distance between the two phos-

(10) Toniolo, C.; Crisma, M.; Bonora, G. M.; Benedetti, E.; Di Blasio, B.; Pavone, V.; Pedone, C.; Santini, A. *Biopolymers* **1991**, *31*, 129−138.
(11) Burgess, A. W.; Ponnuswamy, P. K.; Scheraga, H. A. *Isr. J. Chem.* **1974**, *12*, 239.
(12) Némethy, G.; Scheraga, H. A. *Quart. Rev. Biophys.* **1977**, *10*, 239.
(13) Marshall, G. R.; Bosshard, H. E. *Circ. Res.* **1972**, *30/31 (Suppl. II)*, 143−150.
(14) Hodgkin, E. E.; Clark, J. D.; Miller, K. R.; Marshall, G. R. *Biopolymers* **1990**, *30*, 533.
(15) Burgess, A. W.; Leach, S. J. *Biopolymers* **1973**, *12*, 2599−2605.
(16) Karle, I. L.; Balaram, P. *Biochemistry* **1990**, *29*, 6748.
(17) Marshall, G. R.; Hodgkin, E. E.; Langs, D. A.; Smith, G. D.; Zabrocki, J.; Leplawy, M. T. *Proc. Natl. Acad. Aci. U.S.A.* **1990**, *87*, 487.

phorus atoms. That distance was found to be 6.8 Å. This indicated that metal binding was possible, particularly when one factors in that in the crystal structure the two phosphine sulfides are turned away from each other. This results in the distance in the crystal structure being considerably longer than the potential minimum distance when both phosphorus atoms are free to rotate toward each other.

NMR Structural Data. To determine if the Pps(S)-containing short peptides have the same secondary structure in solution as in the solid phase, and to determine what conformation the peptide backbone has after chelation of transition metals, the secondary structure of peptide **5**, and rhodium complex peptide **7**, were studied by NMR. Before such a study could take place assignment of all the proton chemical shifts in the peptide backbone had to be made.[18−22]

Sequential Assignment of Proton Resonances. The acid terminal groups on the peptides studied were varied for a variety of reasons. We were only able to obtain crystals of the acid terminal peptides, and as a consequence the crystal structure is of an acid terminal peptide. The same peptide was not suitable for the NMR work due to its solubility and the observation that the NMR line shape was broad. For this reason the methyl ester was investigated by NMR. Both the ester and the amide-terminated metal complexes were evaluated. Except for the differences mentioned below, the spectra were qualitatively the similar. The amide data for the complex is presented in the paper because of our ability to resolve and assign all the protons in the molecule.

Proton chemical shifts of peptides **5**, **6**, and **7** were assigned by analysis of TOCSY[23] and NOESY[24] spectra. The Pps(S)^4 and Pps(S)^8 residues were identified by the spin propagation from NH through βH. The N-terminal Ala(1) residue was assigned based on the NOE connection between the acetyl methyl and NH proton of Ala(1). Sequential assignment[18] of all peptides was obtained by using the NH-αH fingerprint region of the NOESY spectrum. All of the $d_{\alpha N}$ connections between adjacent residues were observed. For the Aib residues at 2, 7, and 11, the lost connectivity was restored by observing NOE between Aib-CH_3 and the neighboring NH_{i+1} protons. With the exception of the aromatic protons on the phenyl rings attached to the phosphorus atoms, it was possible to assign all of the proton resonances to specific protons for each residue of the peptides. The complete sequence-specific assignments for peptides **5**, **6**, and **7** are shown in Tables 2, 3, and 4.

The structures for peptides **4**−**7** are as follows:

Ac-Ala-Aib-Ala-Pps(S)-Ala-Ala-Aib-Pps(S)-Ala-Ala-Aib-Ala-OH (**4**).

Ac-Ala-Aib-Ala-Pps(S)-Ala-Ala-Aib-Pps(S)-Ala-Ala-Aib-Ala-Ala-OCH_3 (**5**).

Ac-Ala-Aib-Ala-Pps(S)-Ala-Ala-Aib-Pps(S)-Ala-Ala-Aib-Ala-NH_2 (**6**).

Rhodium complex of Ac-Ala-Aib-Ala-Pps-Ala-Ala-Aib-Pps-Ala-Ala-Aib-Ala-NH_2 (**7**).

Table 2. NMR Assignments for Peptide 5 from TOCSY and NOESY Experiments

	α-H (ppm)	N−H (ppm)	β-H (ppm)
Ala^1	4.21	7.98	1.18
Aib^2		8.39	1.29 and 1.33
Ala^3	3.68	7.97	1.04
Pps(S)^4	4.46	7.77	3.20 and 3.20
Ala^5	4.15	7.59	1.23
Ala^6	4.09	7.58	1.24
Aib^7		7.95	1.12 and 1.08
Pps(S)^8	4.36	7.82	3.28 and 3.19
Ala^9	3.94	7.73	1.26
Ala^{10}	4.01	7.39	1.20
Aib^{11}		7.52	1.23 and 1.26
Ala^{12}	4.16	7.22	1.17
Ala^{13}	4.16	7.77	1.27
AcO	1.81		
OMe	3.31		

Table 3. NMR Assignments for Peptide 6 from TOCSY and NOESY Experiments

	α-H (ppm)	N−H (ppm)	β-H (ppm)
Ala^1	4.20	7.99	1.15
Aib^2		8.40	1.15 and 1.33
Ala^3	3.68	7.90	1.05
Pps(S)^4	4.46	7.77	3.20 and 3.20
Ala^5	4.15	7.58	1.24
Ala^6	4.10	7.58	1.23
Aib^7		7.98	1.13 and 1.09
Pps(S)^8	4.34	7.82	3.28 and 3.18
Ala^9	3.92	7.73	1.27
Ala^{10}	3.96	7.44	1.21
Aib^{11}		7.48	1.26 and 1.22
Ala^{12}	3.96	7.20	1.19
AcO	1.80		
$CONH_2$	6.91 and 6.94		

Table 4. NMR Assignments for Complex 7 from TOCSY and NOESY Experiments

	α-H (ppm)	N−H (ppm)	β-H (ppm)
Ala^1	4.32	8.48	1.25
Aib^2		9.04	1.39 and 1.39
Ala^3	3.84	8.26	1.15
Pps(S)^4	4.32	7.89	2.84 and 3.11
Ala^5	4.31	8.02	1.46
Ala^6	4.04	7.67	1.37
Aib^7		8.28	1.29 and 1.37
Pps(S)^8	4.21	8.24	3.03 and 3.18
Ala^9	3.61	8.14	1.41
Ala^{10}	3.92	7.71	1.34
Aib^{11}		7.57	1.42 and 1.50
Ala^{12}	4.00	7.33	1.21
AcO	1.96		
$CONH_2$	7.04 and 7.12		

NMR Study of the Secondary Structure of Peptide 5. The helical region of a peptide can often be characterized by sequential d_{NN} and medium-range d_{NN} (i, $i+2$) and $d_{\alpha N}$[(i, $i+2$), (i, $i+3$)] NOE connectivities and small values (<6.0 Hz) of $^3J_{HN-\alpha H}$. We have used these methods along with the temperature dependence of the $N-H$ chemical shifts in the characterization of peptides **5** and **7**.

Table 5 summarizes the NOE data for peptide **5** and Scheme 1 illustrates these tabulated NOEs. The sequential d_{NN} (i, $i+1$) observed along the peptide chain is indicative of the peptide having a defined structure. A number of the medium range d_{NN} (i, $i+2$) and $d_{\alpha N}$ (i, $i+2$) were also observed. Although d_{NN} (1, 3) and $d_{\alpha N}$ (8, 10) were missing, the corresponding $d_{\alpha N}$ (1, 3) and d_{NN} (8, 10) could be identified (Scheme 1). The $d_{\alpha N}$ (i, $i+3$) for Ala(3), Ala(6), and Ala(10) were also observed. The observed NOEs, discussed above, particularly the observed $d_{\alpha N}$ (i, $i+2$) and the lack of $d_{\alpha N}$ (i, $i+4$), are

(18) Englander, S. W.; Wand, A. J. *Biochemistry* **1987**, *26*, 5953.
(19) Wüthrich, K.; Wider, G.; Wagner, G.; Braun, W. *J. Mol. Biol.* **1982**, *155*, 311.
(20) Wüthrich, K. *Biopolymers* **1983**, *22*, 131.
(21) Wüthrich, K.; Billeter, M.; Braun, W. *J. Mol. Biol.* **1984**, *180*, 715.
(22) Billeter, M.; Braun, W.; Wüthrich, K. *J. Mol. Biol.* **1982**, *155*, 321.
(23) Bax, A.; Davis, D. G. *J. Magn. Reson.* **1985**, *65*, 355.
(24) Kumar, A.; Ernst, R. R.; Wuthrich, K. *Biophy. Res. Commun.* **1980**, *95*, 1.

Table 5. NMR-Based Inter-residue Distance Constraints for Peptide 5[a]

Ala[1]	Aib[2]	Ala[3]	Pps[4]	Ala[5]	Ala[6]	Aib[7]	Pps[8]	Ala[9]	Ala[10]	Aib[11]	Ala[12]	Ala[13]	
●	●	●	●	●	●	●	●	●	●	●	●	/	d_{NN} (i, $i+1$)
●	/	●	●	●	●	/	●	●	●	/	●	/	$d_{\alpha N}$ (i, $i+1$)
○	●	●	●	●	●	●	●	○	●	○	/	/	d_{NN} (i, $i+2$)
●	/	●	●	●	●	/	○	○	●	/	/	/	$d_{\alpha N}$(i, $i+2$)
○	/	●	○	○	●	/	○	○	●	/	/	/	$d_{\alpha N}$ (i, $i+3$)
○	/	○	○	○	○	/	○	○	/	/	/	/	$d_{\alpha N}$(i, $i+4$)

[a] (●) NOE observed; (○) no NOE observed; (/) not applicable.

Scheme 1. Medium-Range NOEs in Peptide 5

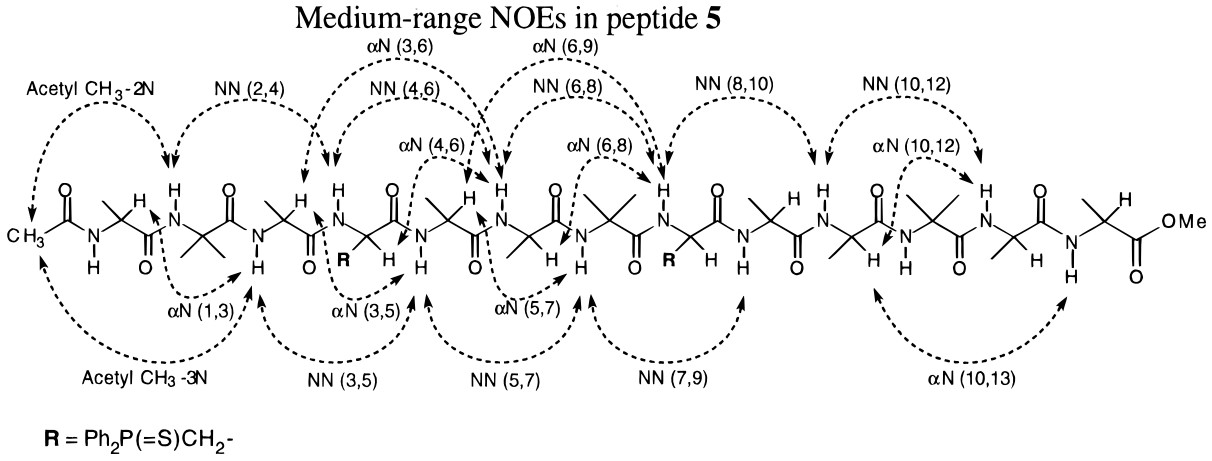

Table 6. Torsion Angle ϕ Derived from $^3J_{\alpha N}$ for Peptide 5

	Ala[1]	Aib[2]	Ala[3]	Pps[4]	Ala[5]	Ala[6]	Aib[7]	Pps[8]	Ala[9]	Ala[10]	Aib[11]	Ala[12]	Ala[13]
$^3J_{\alpha N}$ (Hz)	6.5	/	5.8	6.5	5.9	?	/	6.0	6.5	6.0	/	7.8	6.5
ϕ (deg)	−77	/	−72	−77	−73	?	/	−74	−77	−74	/	−88	−77

Chart 1

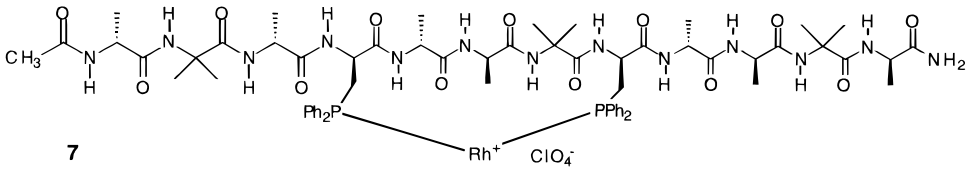

7

consistent with this peptide existing predominately in 3_{10}-helical secondary structure from Ala(1) to Ala(10).[25]

The vicinal coupling constants $^3J_{HN-\alpha H}$ for Ala(1) to Ala(12) (except that of Ala(6) which could not be resolved) were obtained from the one-dimensional ^1H spectrum. The average value of the coupling constants from Ala(1) to Ala(10) was found to be 6.2 Hz (Table 6). This corresponds to an average torsion angle ϕ of −70° (ϕ = −54° was used for Aib(2) and Aib(7) in the calculation), which was within the range of −60° to −90° typically found in helical conformations.[25,26] The absence of NOEs d_{NN} (9, 11) and $d_{\alpha N}$ (9, 11) suggested that Aib(11) may have had a positive torsion angle ϕ, and consequently the acid terminus of the peptide may have been in an extended form. This result was analogous to the solid state structure of peptide **4** in which the end of the structure was found to be in an extended form. The relatively large $^3J_{HN-\alpha H}$ and torsion angle ϕ for Ala(12) were in agreement with the NOE observations and this conclusion.

2D NMR Study of the Secondary Structure of Complex 7. Next, the secondary structure of the rhodium complex **7** (Chart 1) was examined. To date, we have not been able to obtain X-ray quality crystals of any of our phosphine-containing peptides with a transition metal coordinated, so we embarked on determining the secondary structure in solution by NMR.

Complex **7** was chosen for study because of the quality of the NOE data obtained with this peptide. The sequential assignment of the peptide backbone is listed in Table 4. The NMR assignment of this molecule was done in the same manner as described for peptide **5**. The sequential and medium range NOEs are listed in Table 7 and the medium range NOEs are illustrated in Scheme 2. All of the sequential d_{NN} (i, $i+1$) NOEs along the peptide chain were observed, indicating that the peptide backbone had a conformationally defined structure. From Ala(1) to Ala(8), none of the medium range d_{NN} (i, $i+2$), $d_{\alpha N}$ (i, $i+2$), or $d_{\beta N}$ (i, $i+2$) NOEs were found, while all of the $d_{\alpha N}$ (i, $i+3$) interactions were present. This along with the absence of the $d_{\alpha N}$ (i, $i+2$) NOEs is consistent with an ordered structure other than the 3_{10} structure observed for this region in peptide **5**. The lack of $d_{\alpha N}$ (i, $i+4$) suggests a structure other than α-helical as well. The presence of $d_{\alpha N}$ (8, 11), d_{NN} (9, 11), and d_{NN} (10, 12) indicated that Aib(11) had a negative torsion angle ϕ (assumed here to be −54°). This data suggests

(25) Wüthrich, K. *NMR of Proteins and Nucleic Acids*; J. Wiley and Sons: New York, 1986.
(26) Bystrov, V. *Prog. Nucl. Magn. Spectrosc.* **1976**, *10*, 41−82.

Table 7. NMR-Based Inter-residue Distance Constraints for Complex 7[a]

Ala[1]	Aib[2]	Ala[3]	Pps[4]	Ala[5]	Ala[6]	Aib[7]	Pps[8]	Ala[9]	Ala[10]	Aib[11]	Ala[12]	
●	●	●	●	●	●	●	●	●	●	●	/	d_{NN} (i, $i+1$)
●	/	●	●	●	●	/	●	●	●	/	/	$d_{\alpha N}$ (i, $i+1$)
○	○	○	○	○	○	○	○	●	●	/	/	d_{NN} (i, $i+2$)
○	/	/	○	○	○	/	○	○	○	/	/	$d_{\alpha N}$ (i, $i+2$)
○	○	○	○	○	○	○	○	○	○	/	/	$d_{\beta N}$ (i, $i+2$)
●	/	●	●	●	●	/	●	○	/	/	/	$d_{\alpha N}$ (i, $i+3$)
●	○	○	○	○	●	○	○	○	/	/	/	$d_{\beta N}$ (i, $i+3$)
○	/	○	○	○	○	/	○	/	/	/	/	$d_{\alpha N}$ (i, $i+4$)

[a] (●) NOE observed; (○) no NOE observed; (/) not applicable.

Scheme 2. Medium-Range NOEs in Complex 7

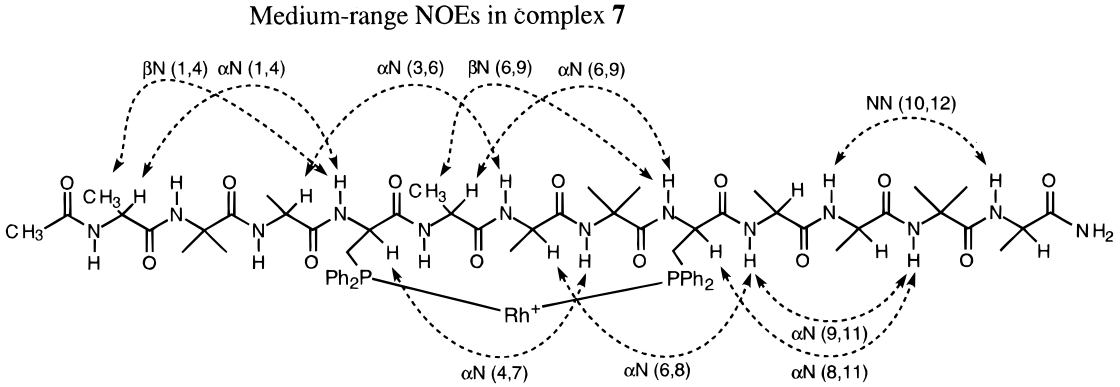

Table 8. Torsion Angle ϕ Derived from $^3J_{\alpha N}$ for Peptide 7

	Ala[1]	Aib[2]	Ala[3]	Pps[4]	Ala[5]	Ala[6]	Aib[7]	Pps[8]	Ala[9]	Ala[10]	Aib[11]	Ala[12]
$^3J_{\alpha N\,(Hz)}$	5.14	/	4.63	6.68	5.60	6.17	/	5.31	4.96	8.00	/	6.85
ϕ (deg)	−70	/	−66	−80	−73	−75	/	−70	−68	−90	/	−80

Table 9. Variable Temperature Experiment on Complex 7[a]

	−10 °C	−5 °C	0 °C	5 °C	10 °C	15 °C	20 °C	$-\Delta\delta/\Delta T$	H-bond
NH Ala[1]	8.52	8.49	8.46	8.44	8.41	8.38	8.35	5.7	○
NH Aib[2]	9.09	9.05	9.01	8.97	8.93	8.88	8.84	8.3	○
NH Ala[3]	8.31		8.27		8.23		8.18	4.1	●
NH Pps[4]	7.93	7.93	7.92	7.92	7.92	7.92	7.91	1.0	●
NH Ala[5]	8.05	8.04	8.02	8.00	7.98	7.96	7.95	3.3	●
NH Ala[6]	7.71		7.68		7.65		7.62	3.0	●
NH Aib[7]	8.33	8.30	8.28	8.30	8.23	8.20	8.18	5.0	○
NH Pps[8]	8.29		8.25		8.21		8.16	4.1	●
NH Ala[9]	8.18	8.17	8.15	8.14	8.13	8.12	8.10	2.7	●
NH Ala[10]	7.75		7.72		7.68		7.62	4.3	●
NH Aib[11]	7.54	7.53	7.53	7.53	7.53	7.52	7.51	1.0	●
NH Ala[12]	7.37		7.35		7.34		7.32	1.1	●

[a] δ_{NH} (ppm) vs temperature (K) and temperature dependencies of amide proton $-\Delta\delta/\Delta T$ (10^{-3} ppm/K) in DMF-d_7. (●) Hydrogen bonded; (○) not hydrogen bonded.

that unlike the acid terminus of peptide **4** in the solid state and the acid terminus of **5** in solution, the amide terminus of complex **7** was in helical form. The d_{NN} (9, 11) and d_{NN} (10, 12) interactions found after the metal binding site are consistent with either a 3_{10} or an α-helical structure.

Crude vicinal coupling constants $^3J_{HN-\alpha H}$ of Ala(1) to Ala(12), except that of Ala(5), were obtained from the one-dimensional ^{1}H spectrum at −10 °C. $^3J_{HN-\alpha H}$ of Ala(5) could not be resolved in this spectrum, but it was resolved in the one-imensional ^{1}H spectrum at 10 °C. All coupling constants $^3J_{HN-\alpha H}$, together with their corresponding torsion angles ϕ, were summarized in Table 8. All torsion angles ϕ obtained were within the range of −60° to −90°. From Ala(1) to Ala(12) the average of the torsion angle ϕ was −69° (again, ϕ = −54° was used for Aib(2) and Aib(7) in the calculation), which was near −60°, the value of ϕ defined for α or 3_{10}-helices.[25,26]

Since the NOE and $^3J_{\alpha N}$ data for peptide **7** were inconclusive, the temperature dependence of the chemical shift of the amide protons, which is often used to indicate the presence of hydrogen bonds in a peptide backbone, was determined. The results are summarized in Table 9. As expected, it was found that amide protons of Ala(1) and Aib(2) were exposed to solvent. In a helical structure there is no internal hydrogen bond acceptor available for these two amide protons, consequently they exhibit a large change in their chemical shift as a function of temperature. The temperature coefficient for the amide proton of Aib(7) ($-\Delta\delta/\Delta T$ = 5) indicated that this proton was also exposed to solvent. This site is located between the two metal binding amino acids and it is possible that binding a metal between the two side chains may strain the helix, resulting in exposure of the amide proton of Aib(7). All the other N−Hs in the molecule were found to be internally hydrogen bonded.

In terms of structural issues other than the peptide secondary structure. The rhodium complex is characterized with norbornadiene as the other ligands in the rhodium. Mass spectrometry shows a strong peak for the

molecular ion corresponding to this complex. On the basis of the lack of a trans P−P coupling, we have assigned the phosphines as being in a cis relationship on the metal.

Discussion

Peptides that contain Aib are known to have a propensity for the formation of either α-helical or 3_{10} helical secondary structures.[13−17,27] We have found that the phosphorus-containing peptides reported in this paper have organized structures which are for the most part helical. Peptides rich in amino isobutyric acid often favor a 3_{10} helical structure, particularly near the amine terminus. Based on the X-ray data and NMR work, this appears to be the case with our peptides as well. The orientation of the amino acids with phosphine metal binding groups in their side chains is i, $i + 4$ to each other. As a consequence of this positioning of these amino acids, the region of the peptide near those amino acids must be in an α-helical conformation for the phosphine to be able to bind rhodium. The crystal structure of peptide **4** revealed that the amine end of the peptide had a 3_{10} helical structure with the secondary structure changing to α-helical in the region where the phosphine sulfides are located. It is interesting that the region of the peptide crystal structure where the phosphine sulfides were located was α-helical. The reason for the switch from 3_{10} helix to α-helix is not clear. One possibility is that an α-helical section is better able to accommodate the extremely large diphenylphosphine side chains. Another possibility is that crystal-packing forces cause the molecule to adopt this conformation. The NMR study of peptide **5** reveals that this peptide exists in primarily a 3_{10} helical structure. This includes the region of the molecule that was α-helical in the X-ray structure of peptide **4**. Despite this molecule having 3_{10} helical structure, after removal of the sulfur atoms this molecule readily acts as a bis-chelating ligand for rhodium. For this to occur the molecule must adopt a conformation other than a 3_{10} helix. One obvious change would be for the peptide to take on an α-helical structure. The NOE data for complex **7** indicates that the region between residues 9−12 is helical. The helical nature of this end of complex **7** could be due to metal binding between the i, $i + 4$ phosphines inducing a helical structure or due to the amide terminus of this peptide. It has been demonstrated that amide-terminated peptides have a greater propensity for helix formation. While it is clear from the NMR data the complex **7** has a stable secondary structure, we were not able to assign that structure as either 3_{10} or α-helical.

The acid terminus of peptides **4** and **5** is in an extended form. This effect has been seen before with Aib rich peptides.[16,17] Both positive and negative values of the torsion angles ϕ and ψ are of equal energy for aminoisobutyric acid; consequently, there was no steric hindrance to Aib(11) adopting positive torsion angles, which lead to an extended structure. The NMR data of complex **7** indicates that the acid terminus of that peptide is helical. This could be due to metal binding but is most likely caused by the fact that this peptide is terminated as the amide. This provides a hydrogen bonding group at the carboxy end of the molecule which is capable of continuing the hydrogen bonding network of the helical peptide.

Conclusion

The differentiation between α-helical and 3_{10} helical structures by NMR is not simple or always conclusive. The observation of short proton−proton distances by NOE is the fundamental tool for this task. While the destination between turns and helical structures is relatively straight forward, the interactions used to distinguish between an α-helix and a 3_{10} helix are weak and sometimes difficult to observe. The presence of NOEs between the α proton of one amino acid and the N−H two residues away is often found in 3_{10} helices. Those two protons are on opposite sides of an α-helix. A similar interaction between the α proton of one amino acid and the N−H of a residue four positions down the peptide chain is often used to demonstrate the presence of α-helical character. In both cases these interactions are weak and can be difficult to observe. In the case of our NMR data peptide **5** gives strong cross peaks from the $\alpha N(i, i + 2)$ interaction, and we use this to assign its structure as primarily a 3_{10} helix. The structure of complex **7** is not as clearly assigned. The NOEs expected for a molecule with an organized structure, $d_{\alpha N}(i, i + 1)$ and $d_{NN}(i, i + 1)$, were found but the crossed peaks necessary for the differentiation between an α or a 3_{10} helix were not observed. To verify that the molecule actually did possess secondary structure, the temperature dependence of the N−H chemical shift was determined. That study revelead that all but one of the expected internal hydrogen bonds were present, and therefore this molecule is likely to have had an organized secondary structure. The reason the N−H of Aib(7) shifts with temperature may be due to an interaction of its hydrogen bond acceptor in the helical scaffold with rhodium or simply that metal binding to that region of the peptide may perturb the structure sufficiently to disrupt the hydrogen bond between N−H and its carbonyl partner.

The structural characterization of phosphorus-containing peptides was carried out. The X-ray and NMR data indicate these peptides have organized structures which are helical in at least two cases. We are in the process of exploring the use of these peptides as ligands for transition metals with a wide variety of goals. These ligands have potential in stereo- and regioselective catalysis with transition metals, as delivery agents for therapeutic and diagnostic metals, and as tools for the investigation of protein structure and folding.

Experimental Section

NMR Spectroscopy. Samples were made by dissolving approximately 10 mg of each peptide in 0.7 mL of DMSO-d_6 or DMF-d_7. The samples were degassed by several freeze-thaw cycles and sealed in NMR tubes under vacuum. All 2D NMR spectra were recorded with a Varian Unity-600 spectrometer operating at 600 MHz, interfaced with a Sun SPARC I computer. The data were processed off-line on a SPARC 10 station with VNMR software.

The total correlation TOCSY spectra were recorded using an MELV-17 mixing sequence of 100 ms, flanked by two 2 ms trim pulses. Phase-sensitive 2D spectra were obtained by employing the Hypercomplex method. A total of $2 \times 256 \times 1024$ data matrix with 16 scans per t_1 value were collected. Gaussian line broadening and sinebell function were used in weighting t_2 and t_1 dimensions, respectively. After two-

(27) Karle, I. L.; Flippen-Anderson, J. L.; Uma, K.; Balaram, P. *Biochemistry* **1989**, *28*, 6696.

dimensional Fourier transform, the spectra resulted in 1K × 1K data points and were phase and baseline corrected in both dimensions. Chemical shifts were measured in parts per million (ppm) downfield from internal TMS, or with the center line of the lower field quintet at 2.90 ppm for DMF-d_7.

The NOESY spectra resulted from a 2 × 512 × 4096 data matrix with 16 scans per t_1 value. The spectra were recorded with a 250 and 450 ms mixing time, but 450 ms generally gave better results. Hypercomplex method was used to yield phase-sensitive spectra. The time domain data were zero filled to yield a 2K × 2K data matrices and were processed in the similar to the TOCSY spectra.

Variable temperature experiments were performed on complex **7**. Chemical shifts were measured in parts per million (ppm) downfield from internal TMS. The temperature dependencies of the amide proton resonances were determined by seven measurements over a range of −10 °C to 20 °C. Four COSY spectra were also taken over this range at 10 °C intervals to help identify amide proton peaks. Each COSY spectrum was collected into a 512 × 4096 data matrix with 16 scans per t_1 value. The time domain data was zero filled to yield a 4096 × 4096 data matrix and was Fourier transformed using sine-bell weighting function in both t_2 and t_1 dimension.

Single Crystal Growth and X-ray Data Collection and Refinement of Peptide 4. A 50 mg amount of peptide **4** was dissolved in 2 mL of methanol, and the solution was filtered through a microfilter (pore size: 5 μm) into a 10 mL crystallization dish. Mixed solvent ethyl acetate/hexane (2 mL, 8−2 by volume) was then added to the dish. The dish was then covered with parafilm into which several holes were made. The solvent was allowed to evaporate overnight without any interruption and single crystals were obtained. The crystals obtained were stable only when surrounded by mother liquor. The crystal was mounted for X-ray with the mother liquor also sealed in the capillary tube.

X-ray Analysis.[30] Crystal data: $[C_{65}H_{88}N_{12}O_{16}P_2S_2]$·EtOAc; formula wt. 1475.64, 0.31 × 0.27 × 0.23 mm, triclinic, a = 37.842(6) Å, b = 10.627(2) Å, c = 20.037(5) Å, Z = 4, density (calcd) = 1.216 g/cm^3. F(000) = 3136, space group $P2_12_12_1$, $R1$ = 0.0893, $wR2$ = 0.2266 for $I > 2\sigma(I)$, goodness of fit = 1.22 for all data. An extinction coefficient of 0.001056 was determined.

A single crystal of **4** was mounted on a glass fiber, cell constants were determined, and intensity data were collected on a Siemens SMART Charge Coupled Device (CCD) Detector system single crystal X-ray diffractometer system. Data were collected at 195 K using graphite monochromated Mo Kα radiation (λ = 0.71073 Å) from a sealed tube X-ray source. A total of 1271 frames of intensity data were collected, with a frame width of 0.3° in ω, and counting time of 10 s/frame. The crystal to detector distance was 6.14 cm, and the total collection time was 6.0 h. Frame integration yielded 45914 reflections, with 12391 unique reflections and 10737 reflections with $I > 2\sigma(I)$. No absorption correction was applied.

Structure solution was determined using SHELXS 86 and refined using SHELXL 93. The structure was solved using Direct Methods, and refinement was carried out using successive full matrix least-squares refinements and difference Fourier map calculations. The acyl end of the peptide exhibited two-fold disorder, with 65%/35% occupancy of the two conformations. Disordered atoms include O9−O13, N12, and C22−C24, and C61. This disorder was linked to a two-fold disorder of S2 (also 65%/35% occupancy.) One phenyl ring bonded to P1 also exhibited a two-fold disorder, where two positions were idealized and refined at ∼60%/40% occupancy. The phenyl ring (C53−C58) and the associated ethyl acetate solvent molecule (O91−O92, C91−C94) were found to be cooperatively disordered, with two orientations at 60%/40% occupancy. The ethyl acetate position constituting 40% occupancy was unresolveable and therefore not included in the structure refinement. All non-hydrogen atoms were refined anisotropically, except for the ethyl acetate atoms, which were refined isotropically. Hydrogen atoms were placed at idealized positions and refined isotropically using the riding model.

Other restraints applied to the refinement were as follows: restraint of the N11−C21, N12′−C22′, N12−C22, and N12′−C23′ bonds to 1.40(1) Å, restraint of the C21−C22, C21−C62, and C21−C61′ bonds to 1.50(1) Å, and restraint of the O11′−C22′ bond to 1.23 Å. In addition, bonds of P2 with C53, C53′, and C47 were restrained to the same value, as were the bonds between P2 and the two disordered S2 positions. The disordered phenyl ring (C53−C58) was refined as a flat regular hexagon, and all bond distances between these atoms were fixed at 1.39 Å. The absolute configuration of the molecule was not determined with certainty from the refinement.

A complete list of displacement coefficients, structure factors, and bond lengths and angles is submitted as Supporting Information.

FMOC-Pps(sulfide)-Ala-OPNB. Ts-Ala-OPNB (1.80 g, 4.93 mmol) was weighed out in a flask. A 150 mL volume of CH_2Cl_2 was added, followed by 3.2 mL (24.6 mmol) of triethylamine. Once the solution became clear it was transferred to a separatory funnel. The solution was washed with water (2 × 50 mL) and brine (50 mL) and dried ($MgSO_4$). After filtration, the solvent was removed on a rotovap. CH_2Cl_2 (100 mL) was then added to the flask, and the solution was cooled to 0 °C. In a second flask, 2.0 g of FMOC-Pps(S)[1] (3.79 mmol) was dissolved in 100 mL of CH_2Cl_2. This solution was cooled to 0 °C and then transferred to the flask containing the CH_2Cl_2 solution of Aib-OPNB. Next EDC (872 mg, 4.55 mmol) and HOBT (614 mg, 4.55 mmol) were added to the reaction mixture, and the reaction was kept at 0 °C under N_2 for 4 h and at rt for 20 h. The reaction mixture was then transferred to a separatory funnel, washed with 1 N HCl (2 × 150 mL), 1 N $NaHCO_3$ (150 mL), water (100 mL), and brine (100 mL) and dried over $MgSO_4$. After filtration and removal of the solvent, the crude product was dried under vacuum. The material was purified by dissolution in a minimum of warm ethyl acetate followed by the addition of enough warm hexane to make the solution cloudy. The solution was allowed to stand at room temperature. Once crystals began to form, the flask was placed in a −20 °C freezer for further crystallization. A 2.33 g amount (84% yield) of the product (FMOC-Pps(S)-Ala-OPNB) was obtained. The product was sufficiently pure to be used directly in the next step.

^{1}H NMR (300 MHz, $CDCl_3$) δ 8.2 (d, J_{HH} = 8.7 Hz, 2H), 7.9−7.8 (m, 4H), 7.76 (d, J_{HH} = 7.4 Hz, 2H), 7.6 (dd, J_{HH} = 10.3 Hz, J_{HH} = 7.4 Hz, 2H), 7.5−7.4 (m, 10H), 7.34−7.28 (m, 2H), 7.15 (d, J_{HH} = 6.7 Hz, 1H), 6.19 (s, 1H), 5.21 (s, 2H), 4.65 (dt, J_{HP} = 21.3 Hz, J_{HH} = 7.1 Hz, 1H), 4.40 (s, 1H), 4.3−4.1 (m, 3H), 3.10 (dd, J_{HP} = 10.5 Hz, J_{HH} = 4.9 Hz, 2H), 1.36 (d, J_{HH} = 7.2 Hz, 3H). ^{13}C NMR (75 MHz, $CDCl_3$) δ 171.7 (s), 170.0 (d, J_{CP} = 10.0 Hz), 155.4 (s), 147.5 (s), 143.5 (s), 142.4 (s), 141.0 (s), 131.8 (d, J_{CP} = 82.0 Hz), 131.7 (s), 130.7 (d, J_{CP} = 10.1 Hz), 128.5 (d, J_{CP} = 12.0 Hz), 128.1 (s), 127.6 (s), 126.9 (s), 125.1 (s), 123.6 (s), 119.8 (s), 67.2 (s), 65.3 (s), 51.0 (s), 48.4 (s), 46.7 (s), 33.4 (d, J_{CP} = 55.7 Hz), 17.56 (s). ^{31}P NMR (120 MHz, $CDCl_3$) δ 39.19. IR (thin film) 3350 (s), 3060 (s), 3003 (m), 2950 (m), 1710 (s), 1700 (s), 1607 (m), 1540 (s), 1438 (m), 1450 (m), 1380 (m), 1220 (m), 1250 (m), 1150 (m), 1105 (m), 1000 (w), 860 (m), 760 (s), 620 (m), 530 (m) cm^{-1}. LRFAB (EI$^+$) m/z (% rel intensity) 734 (MH^+, 100), 718 (18.0), 702 (9.0), 656 (5.0), 635 (7.0), 613 (19.0). HRFAB calcd for $C_{40}H_{36}N_3O_7$-PS (MH^+) m/z 734.20897, measured m/z 734.20900.

FMOC-Pps(sulfide)-Ala-OH (1). Zinc powder (8.93 g, 137 mmol) was added to a solution of 2.00 g (2.73 mmol) of dimer (FMOC-Pps(S)-Ala-OPNB) in 150 mL of acetic acid in water (9:1). After stirring at rt for 1.5 h the mixture was filtered through a plug of Celite. Most of the acetic acid and water were removed under vacuum at 45 °C. The resulting yellowish slurry was then triturated with 500 mL of $CHCl_3$. After filtration, the yellow $CHCl_3$ solution was washed with 1 N aqueous HCl. The $CHCl_3$ solution was further washed with brine (100 mL) and dried ($MgSO_4$). After filtration the solvent was removed on a rotovop. The dimer acid **1** was purified by silica gel chromatography (ethyl acetate:hexane:HOAc = 50:49:1). Product weighed 1.48 g, yield was 91%.

^{1}H NMR (300 MHz, $CDCl_3$) δ 9.30 (s, 1H), 7.86−7.79 (m, 4H), 7.74 (d, J_{HH} = 7.3 Hz, 2H), 7.5 (dd, J_{HH} = 11.2 Hz, J_{HH} = 7.3 Hz, 2H), 7.4−7.2 (m, 11H), 6.32 (d, J_{HH} = 7.8 Hz, 1H), 4.8

(dt J_{HP} = 13.5 Hz, J_{HH} = 6.5 Hz, 1H), 4.3−4.0 (m, 4H), 3.12 (dd, J_{HP} = 10.5 Hz, J_{HH} = 4.9 Hz, 2H), 1.36 (d, J_{HH} = 6.8 Hz, 3H). ^{13}C NMR (75 MHz, $CDCl_3$) δ 175.4 (s), 170.6 (d, J_{CP} = 10.2 Hz), 155.6 (s), 143.5 (s), 141.1 (s), 131.5 (d, J_{CP} = 82.0 Hz), 131.7 (s), 131.0 (d, J_{CP} = 10.4 Hz), 128.5 (d, J_{CP} = 12.5 Hz), 127.7 (s), 127.0 (s), 125.2 (s), 119.9 (s), 67.3 (s), 51.0 (s), 48.5 (s), 46.7 (s), 33.7 (d, J_{CP} = 56.0 Hz), 17.6 (s). ^{31}P NMR (120 MHz, $CDCl_3$) δ 39.16. IR (thin film) 3300 (s), 3050 (s), 3000 (w), 2930 (w), 2350 (m), 1710 (s), 1525 (s), 1480 (w), 1450 (m), 1430 (m), 1400 (w), 1360 (m), 1325 (w), 1250 (s), 1220 (s), 1150 (w), 1100 (m), 1050 (m), 1000 (w), 850 (w), 760 (m), 750 (m), 720 (m), 700 (m), 670 (w), 625 (w), 610 (w), 525 (w), 500 (m) cm^{-1}. LRFAB (EI$^+$) *m*/*z* (% rel intensity) 599 (MH^+, 100), 648 (6.0), 613 (29.0), 583 (15.0), 567 (12.0), 553 (5.0), 522 (5.0), 510 (18.0). HRFAB calcd for $C_{33}H_{31}N_2O_5PS$ (MH^+) *m*/*z* 599.17694, measured *m*/*z* 599.17680.

α-Aminoisobutyric Acid Benzyl Ester *p*-Toluenesulfonate (Ts-Aib-OBn). α-Aminoisobutyric acid (30.0 g, 290 mmol) and *p*-toluenesulfonic acid monohydrate (56.3 g, 296 mmol) were added to a mixture of benzyl alcohol (120 mL) and benzene (60 mL) in a 500 mL round bottom flask. The mixture was heated to reflux, and the water formed in the reaction was trapped in a Dean−Stark receiver. When the reaction stopped evolving water, the mixture was allowed to cool to room temperature. Once at room temperature the mixture was diluted with ether (1000 mL) and cooled in an ice bath for 2 h. The crystalline *p*-toluenesulfonate salt of Aib benzyl ester was collected by filtration, washed with ether (300 mL), and dried in air. After recrystallization from methanol−ether the salt weighed 86.5 g (82% yield).

^{1}H NMR (300 MHz, $CDCl_3$) δ 7.71 (d, J_{HH} = 8.25 Hz, 2H), 7.35 (m, 5H), 7.22 (d, J_{HH} = 7.8 Hz, 2H), 5.22 (s, 2H), 2.34 (s, 3H), 1.55 (s, 6H). ^{13}C NMR (75 MHz, $CDCl_3$) δ 172.59, 143.54, 141.67, 136.46, 129.79, 129.72, 129.53, 126.93, 126.70, 69.26, 57.94, 23.94, 21.29. IR (thin film) 3500 (br m), 3000 (br m), 1800 (s), 1675 (m), 1590 (m), 1350 (w), 1220 (s), 1200 (s), 1150 (m), 1050 (m), 1010 (m), 700 (m) cm^{-1}. MS-FAB (EI$^+$) *m*/*z* (% rel intensity) 559.4 (14), 387.3 (17), 366.2 (MH^+, 9), 387.3 (20), 347.2 (10), 307.2 (8), 194.3 [$(M - C_7H_7O_3S)^+$, 100]. Anal. Calcd for $C_{18}H_{23}O_5NS$ C, 59.16; H, 6.35. Found: C, 58.87; H, 6.51.

FMOC-Ala-Aib-OBn. Ts-Aib-OBn (17.59 g, 48.2 mmol) was weighed into a flask, and $CHCl_3$ (300 mL) was added, followed by 14 mL (24.6 mmol) of triethylamine. Once the mixture turned clear it was transferred to a separatory funnel. The solution was washed with water (2 × 100 mL) and brine (50 mL) and dried ($MgSO_4$). After filtration, the solvent was removed on a rotovap. CH_2Cl_2 (300 mL) was then added to the flask, and the solution was cooled to 0 °C. In a second flask, 10.0 g of FMOC-Ala-OH (32.1 mmol, 1.0 equiv) was dissolved in 200 mL of CH_2Cl_2. This solution was also cooled to 0 °C and then transferred to the flask containing the CH_2Cl_2 solution of Aib-OBn. Next 7.38 g of EDC (38.5 mmol, 1.2 equiv) and 5.2 g of HOBT (38.5 mmol, 1.2 equiv) were added to the reaction mixture. The reaction was kept at 0 °C under N_2 for 4 h and at rt for 20 h. The reaction mixture was then transferred to a separatory funnel, washed with 1 N HCl (2 × 150 mL), 1 N $NaHCO_3$ (150 mL), water (100 mL), and brine (100 mL), and dried over $MgSO_4$. After filtration and removal of the solvent, the crude product was dried under vacuum. A 14.4 g (92% crude yield) amount of the product (FMOC-Ala-Aib-OBn) was obtained. This material was sufficiently pure for use in the next step.

^{1}H NMR (300 MHz, $CDCl_3$) δ 7.76 (d, J_{HH} = 7.7 Hz, 2H), 7.58 (d, J_{HH} = 6.8 Hz, 2H), 7.3 (m, 9H), 6.95 (s, 1H), 5.70 (d, J_{HH} = 7.8 Hz, 1H), 5.14 (s, 2H), 4.35 (d, J_{HH} = 6.9 Hz, 2H), 4.30 (m, 1H), 4.20 (t, J_{HH} = 6.4 Hz, 1H), 1.55 (s, 6H), 1.32 (d, J_{HH} = 6.4 Hz, 3H). ^{13}C NMR (75 MHz, $CDCl_3$) δ 173.9, 171.5, 155.9, 143.6, 141.2, 135.5, 128.4, 128.2, 128.0, 127.7, 127.0, 125.0, 119.9, 67.1, 67.0, 56.4, 50.3, 47.0, 24.6, 18.7. IR (thin film) 3350 (w), 2950 (m), 2830 (w), 1750 (s), 1710 (m), 1700 (s), 1550 (m), 1425 (m), 1380 (m), 1380 (m), 1250 (s), 1150 (w), 800 (w), 790 (m) cm^{-1}. MS-FAB (EI$^+$) *m*/*z* (% rel intensity) 553.9 (8), 487.8 (MH^+, 100), 461.7 (18.0). HRMS calcd for $C_{29}H_{30}O_5N_2$ (MH^+) *m*/*z* 487.22328, measured *m*/*z* 487.22385. Anal. Calcd for $C_{29}H_{30}O_5N_2$: C 69.12; H, 6.07. Found: C, 71.57; H, 6.22.

FMOC-Ala-Aib-OH (2). FMOC-Ala-Aib-OBn (10.0 g, 20.5 mmol) and 0.75 g of 10% Pd-on-carbon were added to a 500 mL round bottom flask containing degassed methanol (200 mL) and equipped with a magnetic stir bar. The air was displaced by nitrogen followed by hydrogen (*via* a H_2 filled balloon), and the reaction mixture was vigorously stirred. The reaction was stopped upon consumption of the starting material, as judged by TLC. After replacement of hydrogen with nitrogen, the flask was opened to air and the catalyst was removed by filtration through Celite. The Celite was washed with 200 mL of methanol, and the solvent was removed *in vacuo*, yielding 7.9 g of **2** (97% yield without purification).

^{1}H NMR (300 MHz, CD_3OD) δ 7.76 (d, J_{HH} = 7.7 Hz, 2H), 7.62 (br m, 2H), 7.36 (dd, J_{HH} = 6.8 Hz, J_{HH} = 6.8 Hz, 2H), 7.28 (dd, J_{HH} = 6.4 Hz, J_{HH} = 6.4 Hz, 2H), 4.34 (m, 2H), 4.18 (t, J_{HH} = 7.1 Hz, 1H), 4.12 (q, J_{HH} = 7.3 Hz, 1H), 1.48 (s, 3H), 1.46 (s, 3H), 1.30 (d, J_{HH} = 7.1 Hz, 3H). ^{13}C NMR (75 MHz, CD_3OD) δ 177.8, 174.6, 158.1, 145.2, 142.5, 128.7, 128.2, 126.2, 120.0, 67.9, 57.0, 51.8, 25.3, 25.0, 18.4. IR (thin film) 3350 (m), 2950 (w), 2900 (w), 2880 (w), 1750 (s), 1650 (s), 1550 (m), 1450 (m), 1280 (m), 1250 (m), 1180 (m), 1150 (w), 800 (m), 790 (m) cm^{-1}. LRFAB (EI$^+$) *m*/*z* (% rel intensity) 397 [$(M + H)^+$, 100], 369 (70), 337 (10), 311 (11). HRFAB calcd for $C_{22}H_{25}O_5N_2$ (MH^+) *m*/*z* 397.17633, measured *m*/*z* 397.17470.

Ac-Ala-Aib-Ala-OBn. A solution of the *N*-carboxyanhydride of α-aminoisobutyric acid[28] (10.1 g, 78.3 mmol) in 250 mL of THF was cooled, under N_2, to −78 °C. This solution was then slowly added via cannula to a stirred solution of Et_3N (22 mL, 156.6 mmol) and alanine benzyl ester *p*-toluenesulfonate (26.4 g, 78.3 mmol) in 300 mL of CH_2Cl_2 at −78 °C. The mixture was stirred at −78 °C for 10 min and then slowly warmed to room temperature. After stirring at room temperature for about 30 min, approximately 80% of the solvent was removed, and the oily mixture was placed in −20 °C freezer for several hours. The triethylamine salt was removed by filtration of the cold mixture through a fritted funnel. The remaining solvent was removed under vacuum. The crude product, Aib-Ala-OBn, was immediately used in the next coupling reaction.

The crude Aib-Ala-OBn dimer was dissolved in 150 mL of CH_2Cl_2 and cooled to 0 °C. After cooling, the solution was transferred to a 0 °C CH_2Cl_2 (200 mL) solution of Ac-Ala-OH (6.88 g, 52.5 mmol) in a 500 mL round bottom flask. Next, 15.2 g of DCC (73.5 mmol) and 8.5 g of HOBT (63.0 mmol) were added to this mixture, and the reaction was kept at 0 °C under N_2 for 4 h and at rt for 20 h. The reaction mixture was then transferred to a separatory funnel, washed with 1 N HCl (2 × 50 mL), 1 N $NaHCO_3$ (50 mL), water (50 mL), and brine (50 mL), and dried over $MgSO_4$. After filtration and removal of the solvent under vacuum, the crude product was purified by silica gel chromatography (75:25 ethyl acetate:hexane, R_f = 0.3), yielding 11.9 g of Ac-Ala-Aib-Ala-OBn (60% yield).

^{1}H NMR (300 MHz, $CDCl_3$) δ 7.35 (br m, 5H), 6.98 (d, J_{HH} = 7.1 Hz, 1H), 6.70 (s, 1H), 6.13 (d, J_{HH} = 6.4 Hz, 1H), 5.16 (dd, J_{HH} = 12.0 Hz, J_{HH} = 24.0 Hz, 2H), 4.58 (dq, J_{HH} = 7.3 Hz, J_{HH} = 7.1 Hz, 1H), 4.32 (dq, J_{HH} = 6.8 Hz, J_{HH} = 7.1 Hz, 1H), 1.99 (s, 3H), 1.57 (s, 3H), 1.50 (s, 3H), 1.40 (d, J_{HH} = 7.1 Hz, 3H), 1.33 (d, J_{HH} = 6.8 Hz, 3H). ^{13}C NMR (75 MHz, $CDCl_3$) δ 173.5, 172.9, 171.9, 170.5, 135.4, 128.6, 128.4, 128.1, 67.0, 57.2, 49.7, 48.4, 25.9, 24.5, 23.1, 17.9, 17.6. IR (thin film) 3350 (br w), 2950 (br m), 1750 (s), 1650 (m), 1550 (br w), 1400 (m), 1350 (s), 1150 (w), 900 (w) cm^{-1}. LRFAB (EI+) *m*/*z* (% rel intensity) 378 (MH^+, 100), 369 (50), 336 (5), 317 (12). HRFAB calcd for $C_{19}H_{27}O_5N_3$ (MH^+) *m*/*z* 378.20288, measured *m*/*z* 378.20340.

Ac-Ala-Aib-Ala-OH (3). Ac-Ala-Aib-Ala-OBn (1.83 g, 4.85 mmol) and 0.3 g of 10% Pd-on-carbon were added to a 250 mL round bottom flask of degassed methanol (100 mL) equipped with a magnetic stirrer. The air was displaced by nitrogen followed by hydrogen (via a H_2 filled balloon), and the reaction mixture was vigorously stirred. The reaction was stopped

(28) Hanby, W. E.; Waley, S. G.; Watson, J. *J. Chem. Soc.* **1950**, 3009.

upon consumption of the starting material, as judged by TLC. After replacement of hydrogen with nitrogen the flask was open to air, and the reaction mixture was filtered through Celite to remove the catalyst. The Celite was washed with 200 mL of methanol. The solvent was removed *in vacuo*, yielding 1.36 g of **3** (crude yield 98%).

^{1}H NMR (300 MHz, DMSO-d_6) δ 8.14 (br s, 1H), 8.12 (s, 1H), 7.41 (d, J_{HH} = 6.5 Hz, 1H), 4.10 (m, 2H), 1.81 (s, 3H), 1.34 (s, 3H), 1.31 (s, 3H), 1.19 (d, J_{HH} = 6.3 Hz, 3H), 1.14 (d, J_{HH} = 6.4 Hz, 3H). ^{13}C NMR (75 MHz, DMSO-d_6) δ 174.0, 173.5, 172.3, 169.6, 55.8, 49.0, 47.8, 26.0, 23.9, 22.3, 17.2, 17.1. IR (thin film) 3300 (w), 3000 (w), 2950 (m), 2880 (w), 1750 (s), 1650 (m), 1550 (br w), 1450 (br w), 1350 (s), 1210 (s), 1120 (w) cm^{-1}. LRFAB (EI$^+$) *m*/*z* (% rel intensity) 378 (MH$^+$, 100), 369 (50), 336 (5), 317 (12). HRFAB calcd for $C_{12}H_{21}O_5N_3$ (MH$^+$) *m*/*z* 288.15593, measured *m*/*z* 288.15870.

General Cleavage Procedure (RapidAmide, Wang and Rink Resins based on 0.1 mmol of resin). The resin was soaked in methanol for 1 min and then drained (three times). For cleavage of RapidAmide and Wang resins, after drying for 10 min, 90% trifluoroacetic acid (TFA), 5% 1,2 ethanedithiol (EDT), and 5% water were added. The reaction mixture was agitated for 16 h for RapidAmide resin or 1 h for Wang resin. For Rink resin, after drying for 10 min, 50% (v/v) TFA/CH_2Cl_2 was added, and the resin was stirred for 2 min. After reaction, the TFA solution was removed by filtration, and the resin was washed with 0.5 mL of reaction solution. The volume of TFA was reduced to 1−2 mL under a stream of nitrogen. The crude peptide was then precipitated by addition of 25 mL of diethyl ether followed by cooling to −78 °C. The ether layer was removed and crude peptide was dried under vacuum. The crude peptide was then purified by reverse-phase HPLC.

Ac-Ala-Aib-Ala-Pps(S)-Ala-Ala-Aib-Pps(S)-Ala-Ala-Aib-Ala-OH (4). Small Scale Synthesis. This peptide was synthesized by the standard solid phase FMOC protocol.[29] FMOC-Ala-Wang resin (0.2 mmol equiv total) was used. All couplings were complete in 2 h. Cleavage of the completed peptide from resin was performed according to the procedures described above. The peptide was purified by HPLC. HPLC conditions were the following: column: 22.5-mm × 25-cm ECONOSIL C18 10U; eluent: gradient flow of 95% of solvent B (99% H_2O/1% TFA) and 5% of solvent A (10% H_2O/89% CH_3CN/1% TFA) to 5% of solvent B and 95% of solvent A over 60 min.; flow rate: 8 mL/min.; retention time of peptide **1**: 49.0 min. After HPLC purification, 144 mg of the peptide **4** was obtained. Yield was 52% relative to 0.2 mmol resin used.

Large Scale Synthesis. A 4.45 g amount of FMOC-Ala-Wang resin was used (2.4 mmol equiv). A 4.8 mmol amount of each short peptide residue was used per coupling (1.9 g of FMOC-Ala-Aib-OH; 2.9 g of FMOC-Pps(S)-OH; 1.4 g of Ac-Ala-Aib-Ala-OH). A 4.5 h period was allowed for each coupling step. After all the couplings were complete, the peptide was cleaved from the resin by adding 60 mL of a solution of 90% TFA, 5% 1, 2-ethanedithiol (EDT), and 5% water to the schlink funnel which was then shaken for 30 min. The solution was filtered into a 250 mL round bottom flask, and the resin was rinsed with 20 mL of TFA. The filtrate was concentrated on a rotovap. The residue was dissolved in 100 mL of CH_2Cl_2 and washed with water (50 mL) and brine (50 mL). The CH_2Cl_2 was then removed under vacuum. The oily product was dissolved in a minimum amount of CH_3CN. The solvent was then allowed to evaporate at room temperature until a white solid started to precipitate. The flask was then capped and moved into a −20 °C freezer for further crystallization. The crystals were filtered and vacuum dried (weight 2.1 g). The mother liquor was subjected to HPLC purification (HPLC conditions were the same as those used in purification of peptide **4** from small scale synthesis). The combined peptide fractions weighed 0.6 g. Total yield was 81% relative to 2.4 mmol resin used.

^{1}H NMR (300 MHz, $CDCl_3$) δ 7.90 (br m, 19H), 7.40 (br m, 13H), 4.35 (br m, 4H), 4.10(m, 1H), 3.95 (m, 2H), 3.62 (m, 1H), 3.40 (m, 1H), 3.10 (br m, 4H), 2.05 (s, 3H), 1.50 (br m, 39H). ^{31}P NMR (120 MHz, DMSO-d_6) δ 39.98, 39.59. IR (thin film) 3350 (w), 3325 (br s), 3075 (w), 2990 (w), 2950 (w), 1675 (s), 1550 (s), 1425 (m), 1220 (m), 1180 (s), 1110 (w), 710 (w), 700 (w), 600 (w) cm^{-1}. LRFAB (EI$^+$) *m*/*z* (% rel intensity) 1409 [(M + Na)$^+$, 100], 1387 (MH$^+$, 10), 1379 (30), 1332 (40), 1298 (32). HRFAB calcd for $C_{65}H_{88}O_{14}N_{12}P_2S_2$ (MNa$^+$) *m*/*z* 1409.53570, measured *m*/*z* 1409.53650.

Ac-Ala-Aib-Ala-Pps(S)-Ala-Ala-Aib-Pps(S)-Ala-Ala-Aib-Ala-Ala-OCH$_3$ (5). Peptide **4** (1.69 g, 1.22 mmol) was dissolved in 100 mL of CH_2Cl_2 in a 200 mL round bottom flask, and the solution was cooled to 0 °C. To this solution were added HCl·Ala-OMe (0.85 g, 1.22 mmol), morpholine (1.35 mL, 6.01 mmol), EDC (1.17 g, 6.01 mmol) and HOBT (0.66 g, 6.01 mmol). The reaction was stirred under N_2 at 0 °C for 4 h and at room temperature for 20 h. The reaction mixture was then transferred to a separatory funnel, washed with 1 N HCl (2 × 30 mL), 1 N $NaHCO_3$ (30), water (30 mL), and brine (30 mL), and dried over $MgSO_4$. The solvent was removed under vacuum. The crude product was then dissolved in a minimum amount of CH_3CN in a 100 mL flask. The solvent was allowed to evaporate at room temperature until a white solid started to precipitate. The flask was capped and moved into a −20 °C freezer for further crystallization. The crystals were filtered and placed in vacuum, and the mother liquor was subjected to HPLC purification. HPLC conditions were the following: column: 22.5-mm × 25-cm ECONOSIL C18 10U; eluent: gradient flow of 95% of solvent B (99% H_2O/1% TFA) and 5% of solvent A (10% H_2O/89% CH_3CN/1% TFA) to 5% of solvent B and 95% of solvent A over 60 min.; flow rate: 8 mL/min.; retention time of peptide **5**: 55.4 min. The total peptide weighed 1.17 g (66% yield).

^{1}H NMR (600 MHz, DMSO-d_6) δ 8.39 (s, 1H), 7.98 (d, J_{HH} = 6.5 Hz, 1H), 7.95 (s, 1H), 7.90 (d, J_{HH} = 5.8 Hz, 1H), 7.86 (m, 6H), 7.82 (d, J_{HH} = 6.0 Hz, 1H), 7.77 (d, J_{HH} = 6.5 Hz, 2H), 7.73 (d, J_{HH} = 6.5 Hz, 1H), 7.59 (d, J_{HH} = 6.5 Hz, 1H), 7.58 (m, 1H), 7.51 (m, 15H), 7.39 (d, J_{HH} = 6.0 Hz, 1H), 7.22 (d, J_{HH} = 7.8 Hz, 1H), 4.46 (m, 1H), 4.36 (m, 1H), 4.21 (dq, J_{HH} = 6.5 Hz, J_{HH} = 7.2 Hz, 1H), 4.16 (m, 3H), 4.09 (m, 1H), 4.01 (dq, J_{HH} = 6.0 Hz, J_{HH} = 6.5 Hz, 1H), 3.94 (dq, J_{HH} = 6.5 Hz, J_{HH} = 7.6 Hz, 1H), 3.68 (dq, J_{HH} = 5.8 Hz, J_{HH} = 7.5 Hz, 1H), 3.31 (s, 3H), 3.20 (m, 2H), 3.24 (m, 2H), 1.81 (s, 3H), 1.33 (s, 3H), 1.29 (s, 3H), 1.27 (m, 6H), 1.26 (s, 3H), 1.24 (m, 9H), 1.20 (d, J_{HH} = 7.2 Hz, 3H), 1.18 (m, 6H), 1.12 (s, 3H), 1.08 (s, 3H), 1.04 (d, J_{HH} = 7.5 Hz, 3H). ^{31}P NMR (120 MHz, $CDCl_3$) δ 39.86, 39.48. IR (thin film) 3350 (w), 3325 (br s), 3075 (w), 2990 (w), 2950 (w), 1675 (s), 1550 (s), 1425 (m), 1220 (m), 1110 (w), 710 (w), 700 (w), 600 (w) cm^{-1}. LRFAB (EI$^+$) *m*/*z* (% rel intensity) 1494.6. [(M + Na)$^+$, 100], 1478.7 (24), 1426.7 (13), 1451.6 (5). HRFAB calcd for $C_{69}H_{95}O_{15}N_{13}P_2S_2$ (MNa$^+$) *m*/*z* 1494.58845, measured *m*/*z* 1494.58850.

The proton assignments for the peptide sequence were make by 2D NMR (TOCSY, NOESY) and are listed in Table 2.

Ac-Ala-Aib-Ala-Pps(S)-Ala-Ala-Aib-Pps(S)-Ala-Ala-Aib-Ala-NH$_2$ (6). Both RapidAmide and Rink resins were used in the synthesis of this peptide (0.2 mmol). The peptide was synthesized by the standard solid phase coupling using pentafluorophenol-activated amino acids. All couplings were complete in 2 h. Cleavage of the completed peptide from the resins was according to the procedures described above. The peptide was purified by HPLC under the following conditions: column: 22.5-mm × 25-cm ECONOSIL C18 10U; eluent: gradient flow of 95% of solvent B (99% H_2O/1% TFA) and 5% of solvent A (10% H_2O/89% CH_3CN/1% TFA) to 5% of solvent B and 95% of solvent A over 60 min; flow rate: 8 mL/min.; retention time of peptide **6**: 54.6 min. After HPLC purification, 139 mg of the peptide **6** was obtained using FMOC-Ala-RaMPS resin (50% yield), and 101 mg of the same peptide was obtained using Rink resin (36% yield).

^{1}H NMR (600 MHz, DMSO-d_6) δ 8.40 (s, 1H), 7.99 (d, J_{HH} = 6.9 Hz, 1H), 7.98 (s, 1H), 7.82 (m, 11H), 7.77 (d, J_{HH} = 7.6 Hz, 1H), 7.73 (d, J_{HH} = 6.5 Hz, 1H), 7.60 (m, 15H), 7.44 (d,

(29) Bodanszky, M.; Bodanszky, A. *The Practice of Peptide Synthesis*; Springer-Verlag: Berlin, 1984.

(30) The author has deposited atomic coordinates for this structure with the Cambridge Crystallographic Data Centre. The coordinates can be obtained, on request, from the Director, Cambridge Crystallographic Data Centre, 12 Union Road, Cambridge, CB2 1EZ, UK.

J_{HH} = 6.5 Hz, 1H), 7.20 (d, J_{HH} = 7.2 Hz, 1H), 6.94 (s, 1H), 6.91 (s, 1H), 4.47 (br m, 1H), 4.34 (m, 1H), 4.22 (m, 1H), 4.15 (m, 1H), 4.10 (m, 1H), 3.97 (m, 2H), 3.93 (m, 1H), 3.68 (m, 1H), 3.30 (br m, 4H), 1.81 (s, 3H), 1.20 (br m, 39H). ^{31}P NMR (120 MHz, $CDCl_3$) δ 39.46, 39.16. IR (thin film) 3350 (w), 3325 (br s), 3075 (w), 2990 (w), 2950 (w), 1800 (m), 1775 (w), 1675 (s), 1550 (s), 1425 (m), 1220 (m), 1180 (s), 1110 (w), 710 (w), 700 (w), 600 (w) cm^{-1}. LRFAB (EI$^+$) *m/z* (% rel intensity) 1408.5 [(M + Na)$^+$, 28], 1386.4 (MH$^+$, 24), 1369.4 [(M − H_2O)$^+$, 100],1298.3 (65), 1213.4 (25), 1142.5 (13), 784.4 (87), 699.3 (67), 628.3 (52), 557.3 (38). HRFAB calcd for $C_{65}H_{89}O_{13}N_{13}P_2S_2$ (MNa$^+$) *m/z* 1408.55168, measured *m/z* 1408.55180.

The assignment of the protons was made by 2D NMR (TOCSY, NOESY) and is listed in Table 3.

Ac-Ala-Aib-Ala-Pps-Ala-Ala-Aib-Pps-Ala-Ala-Aib-Ala-NH_2. Raney nickel (300 mg) was washed with degassed methanol (3 × 2 mL) and then transferred, using 3 mL of methanol, into a 25 mL Schlenk tube containing 21 mg (15 μmol) of peptide **6**. The mixture was pump-thaw degassed (three cycles) and was stirred for 12 h at 48 °C. After cooling to room temperature, the reaction mixture was filtered under N_2 into a 10 mL two-neck round bottom flask. Degassed methanol (10 mL) was used to rinse the Raney nickel, and the solvent was removed *in vacuo*. ^{31}P NMR was used to monitor the course of the desulfurization. The reduced peptide was immediately used in the next step. ^{31}P NMR (120 MHz, CD_3OD) δ −20.85, −23.79.

Rhodium Complex of Ac-Ala-Aib-Ala-Pps-Ala-Ala-Aib-Pps-Ala-Ala-Aib-Ala-NH_2 (7). [Rh(NBD)Cl]$_2$ (3.46 mg, 7.5 μmol) and $AgClO_4$ (3.11 mg, 15.0 μmol) were weighed into a 1 mL vial containing a small stir bar. Degassed MeOH (0.50 mL) was added, and the mixture was stirred under N_2 for 15 min. The precipitated AgCl was then filtered off through a microfilter (pore size: 45 μm), and the filtrate was added to the two-neck round bottom flask containing the diphosphine peptide. The solution was stirred under N_2 for 10 min during which time the color of the solution turned from yellow to orange. Methanol solvent was then removed *in vacuo*. The complex was purified by silica gel chromatography. A column of 15 mL of silica gel was capped with a septum, and 100 mL of degassed CH_2Cl_2 was passed through the column before crude complex **7** was loaded. The column was then eluted with 30 mL of degassed CH_2Cl_2 followed by 50 mL of degassed CH_3-OH. The yellow methanol fraction was collected, and solvent was removed *in vacuo*.

^{1}H NMR (600 MHz, DMF-d_7) δ 9.04 (s, 1H), 8.48 (d, J_{HH} = 5.14 Hz, 1H), 8.28 (s 1H), 8.26 (d, J_{HH} = 4.63 Hz, 1H), 8.24 (d, J_{HH} = 5.31 Hz, 1H), 8.14 (d, J_{HH} = 4.96 Hz, 1H), 8.02 (d, J_{HH} = 5.60 Hz, 1H), 7.89 (d, J_{HH} = 6.68 Hz, 1H), 7.71 (d, J_{HH} = 8.00 Hz, 1H), 7.67 (d, J_{HH} = 6.17 Hz, 1H), 7.62 (br m, 11H), 7.57 (s, 1H), 7.45 (m, 14H), 7.33 (d, J_{HH} = 6.85 Hz, 1H), 7.04 (s, 1H), 7.12 (s, 1H), 4.32 (m, 1H), 4.31 (m, 1H), 4.21 (m, 1H), 4.04 (m, 1H), 4.00 (m, 1H), 3.92 (m, 1H), 3.86 (m, 1H), 3.84 (m, 1H), 3.64 (s, 3H), 3.61 (s, 3H), 3.61 (m, 1H), 3.18 (m, 1H), 3.03 (m, 1H), 3.11 (m, 1H), 2.84 (br m, 1H), 1.96 (s, 3H), 1.20 (br m, 39H) cm^{-1}. ^{31}P NMR (120 MHz, CD_3OD) δ 27.24 (d, J_{Rh-P} = 168.0 Hz, 1P), 23.85 (d, J_{Rh-P} = 168.0 Hz, 1P). MS-FAB (EI$^+$) *m/z* (% rel intensity) 1516.9 [(M + H)$^+$ with NBD coordinated to the rhodium (43)], 1426.5 (87), 1334.7 (40), 1241.5 (20), 1179.5 (35), 1108.5 (30), 978.5 (100), 868.5 (22), 609.2 (23), 522.5 (37).

The assignment of the protons was made by 2D NMR (TOCSY, NOESY) and is listed in Table 4.

Acknowledgment. This work was supported by the donors of the Petroleum Research Fund, administered by the American Chemical Society. We gratefully acknowledge the Washington University High-Resolution NMR Facility, partially supported by NIH 1S10R02004, and the Washington University Mass Spectrometry Resource Center, partially supported by NIHRR00954, for their assistance.

JO970773E